tion data collected at low temperature can provide quantitative descriptions of the deformation density in crystals.

- the deformation density at the O atoms shows steep features which cannot be obtained from X-ray diffraction data up to sin $\theta/\lambda = 1{\cdot}06$ Å^{-1}. In this case atomic parameters of a neutron diffraction study are required.

- spatial partitioning of the electron density using the fuzzy-boundary integration is inadequate for alkaline atoms; for H atoms useful results are obtained, provided contracted atomic basis functions ($\kappa_H = 1{\cdot}4$) are used.

- dipole moments for hydrate molecules range from 1·6 to 2·4 D, depending on the partitioning model used. Thus the method is too crude to estimate changes in the dipole moment on crystal formation.

References

BAERT, F., COPPENS, P., STEVENS, E. D. & DEVOS, L. (1982). *Acta Cryst.* A**38**, 143-151.

BATS, J. W., COPPENS, P. & KOETZLE, T. F. (1977). *Acta Cryst.* B**33**, 37-45.

BECKER, P. J. & COPPENS, P. (1974). *Acta Cryst.* A**30**, 129-147.

COPPENS, P. (1975). *Phys. Rev. Lett.* **34**, 98-100.

COPPENS, P., GURU ROW, T. N., LEUNG, P., STEVENS, E. D., BECKER, P. & YOUNG, Y. W. (1979). *Acta Cryst.* A**35**, 63-72.

EISENSTEIN, M. & CRUICKSHANK, D. W. J. (1985). To be published.

ELERMAN, Y., BATS, J. W. & FUESS, H. (1983). *Acta Cryst.* C**39**, 515-518.

FUKAMACHI, T. (1971). Tech. Rep. Ser. *B*, No. 12. Institute for Solid State Physics, Univ. of Tokyo, Japan.

HANSEN, N. K. & COPPENS, P. (1978). *Acta Cryst.* A**34**, 909-921.

HERMANSSON, K. & OLOVSSON, I. (1984). *Theor. Chim. Acta*, **64**, 265-276.

HERMANSSON, K., THOMAS, J. O. & OLOVSSON, I. (1984). *Acta Cryst.* C**40**, 335-340.

HIRSHFELD, F. L. (1977). *Isr. J. Chem.* **16**, 198-201.

HIRSHFELD, F. L. & HOPE, H. (1980). *Acta Cryst.* B**36**, 406-415.

KIRFEL, A. & WILL, G. (1980). *Acta Cryst.* B**36**, 512-523.

KIRFEL, A. & WILL, G. (1981). *Acta Cryst.* B**37**, 525-532.

MOSS, G. (1982). *Electron Distribution and the Chemical Bond*, edited by P. COPPENS & M. B. HALL, pp. 383-411. New York: Plenum.

STEVENS, E. D. & COPPENS, P. (1980). *Acta Cryst.* B**36**, 1864-1876.

TENG, S. T., FUESS, H. & BATS, J. W. (1981). *Z. Kristallogr.* **154**, 337-338.

TENG, S. T., FUESS, H. & BATS, J. W. (1984). *Acta Cryst.* C**40**, 1785-1787.

Acta Cryst. (1986). B**42**, 32-39

Structures of the Basic Zinc Sulfates $3Zn(OH)_2.ZnSO_4.mH_2O$, $m = 3$ and 5

BY I. J. BEAR, I. E. GREY,* I. C. MADSEN, I.E. NEWNHAM AND L. J. ROGERS

CSIRO Division of Mineral Chemistry, PO Box 124, *Port Melbourne, Victoria* 3207, *Australia*

(*Received* 5 *April* 1985; *accepted* 16 *August* 1985)

Abstract

The basic zinc sulfate $3Zn(OH)_2.ZnSO_4.5H_2O$ has triclinic symmetry, $P\bar{1}$, $a = 8{\cdot}354(2)$, $b = 8{\cdot}350(2)$, $c = 11{\cdot}001(2)$ Å, $\alpha = 94{\cdot}41(2)$, $\beta = 82{\cdot}95(2)$, $\gamma = 119{\cdot}93(2)°$, $Z = 2$, $M_r = 549{\cdot}54$, $V = 659{\cdot}9(3)$ Å^3, $D_x = 2{\cdot}77$ g cm^{-3}, λ(Mo $K\bar{\alpha}$) = 0·71069 Å, $\mu = 75{\cdot}54$ cm^{-1}, $F(000) = 544$. Dehydration at room temperature in the water-vapour-pressure range pH_2O = 1-5 mm (~10-50 Pa) gives the trihydrate, $3Zn(OH)_2.ZnSO_4.3H_2O$, symmetry $I\bar{1}$, $a = 8{\cdot}367(3)$, $b = 8{\cdot}393(3)$, $c = 18{\cdot}569(5)$ Å, $\alpha = 90{\cdot}29(3)$, $\beta = 89{\cdot}71(3)$, $\gamma = 120{\cdot}53(3)°$, $Z = 4$, $M_r = 513{\cdot}54$, $V = 1123{\cdot}2(6)$ Å^3, $D_x = 3{\cdot}04$ g cm^{-3}, $\mu = 88{\cdot}52$ cm^{-1}, $F(000) = 1008$. The structures were refined to final wR values of 0·031 and 0·13 for the pentahydrate and the trihydrate respectively, using 2319 and 1120 independent reflections with $I > 3\sigma(I)$. The structures of both compounds comprise modified $Zn(OH)_2$ layers, alternating with layers of water molecules along **c**. The modified $Zn(OH)_2$ layers are CdI_2-type sheets of edge-shared octahedra, with one-seventh of the octahedral sites vacant and with composition $[Zn_6\square(OH)_{12}O_2]^{4-}$. Tetrahedrally coordinated Zn atoms, $[Zn(OH)_3H_2O]^{1-}$, are located above and below the empty sites and corner-share their basal hydroxides with six octahedra. Sulfate groups connect on either side of the octahedral sheets by corner sharing. The composition of the complete neutral layer is $[Zn_6^{VI}\square(OH)_6.Zn_2^{IV}(OH)_6(H_2O)_2.(SO_4)_2]$. The layers are held together by strong hydrogen bonding between the coordinated and free water molecules and the basal O atoms of the sulfate groups. A dehydration mechanism is proposed.

1. Introduction

Basic zinc sulfates have been studied for more than 150 years (Kuhn, 1830) and during this time a vast literature has accumulated on the characterization of a wide range of salts with the general formula $nZn(OH)_2.ZnSO_4.mH_2O$, $1 \le n \le 7$ and $0 \le m \le 5$,

* Author to whom correspondence should be addressed.

0108-7681/86/010032-08$01.50

e.g. see Pascal (1962). There has been considerable controversy as to whether the proposed formulations correspond to pure phases or to mixtures, with one of the most recent studies classifying the basic zinc sulfates as Berthollide compounds, *i.e.* with variable, non-integral ranges of n and m (Jacob & Riquier, 1969). The only salt that has been characterized by a single-crystal structure determination is $Zn(OH)_2.ZnSO_4$ (Iitaka, Oswald & Locchi, 1962).

During the course of a study on the cementation of lead from lead sulfate slurries using zinc as a precipitant, we noted the occurrence of unknown reflections in the X-ray diffraction pattern of the cemented products. A compound with a diffraction pattern that included the unknown reflections was subsequently isolated and analysed and shown to be a basic zinc sulfate of composition $3Zn(OH)_2.ZnSO_4.5H_2O$. A salt with this formula was first reported by Reindel (1869) and was subsequently reported to be the equilibrium composition in the system $ZnO-SO_3-H_2O$ at 298 K, by Fridman (1935). Suitable conditions were established for growing crystals large enough for a structure determination. We report here the results of the structure determination and refinement of both the pentahydrate phase and the trihydrate, $3Zn(OH)_2.ZnSO_4.3H_2O$, prepared by dehydration of the pentahydrate.

2. Experimental

2.1. $3Zn(OH)_2.ZnSO_4.5H_2O$

2.1.1. *Preparation and precession XRD studies.* Transparent crystals of the pentahydrate phase were grown at room temperature from $0{\cdot}5M$ $ZnSO_4$ solution containing metallic Zn powder. The crystals formed loose aggregates of hexagonal platelets on the metal grains. Considerable care had to be taken in handling the crystals as they partially dehydrated at room temperature in low-humidity conditions and exfoliated during exposure to X-rays. This could be avoided by maintaining them in a saturated water-vapour atmosphere. All X-ray diffraction studies were thus carried out while maintaining a flow of water-saturated nitrogen gas over the crystals.

Precession photographs displayed a pronounced pseudohexagonal substructure with corresponding real-space cell parameters $a \approx 3{\cdot}15$, $c \approx 11$ Å. The basal-plane dimension is similar to that for α-$Zn(OH)_2$, 3·14 Å (Feitknecht, 1933*a*), and is consistent with the structure being based on an alternation of $Zn(OH)_2$ and salt layers, as originally proposed by Feitknecht (1933*b*). A number of weaker reflections were observed that could be indexed using an 8·35 Å pseudohexagonal superstructure that was related to the subcell by the relationship $(a, b, c) = (310, \bar{1}20, 001)(a, b, c)_{subcell}$, as shown in Fig. 1. The superstructure a and b parameters are the same as those determined by Jacob & Riquier (1969), from electron diffraction studies on their phase II, $(2{\cdot}5$–$3{\cdot}5)Zn(OH)_2.ZnSO_4.(2$–$2{\cdot}2)H_2O$, and phase III, $(3{\cdot}4$–$4)Zn(OH)_2.ZnSO_4.(2{\cdot}3$–$2{\cdot}8)H_2O$. Series of precession photographs obtained by rotation about the pseudohexagonal c^* axis showed that the true symmetry was triclinic. The single-crystal diffraction patterns were used to index the X-ray powder pattern and accurate cell parameters, obtained from the refinement of the 2θ values of 71 reflections in the range 16–75° (Cu $K\alpha$ radiation), are given in the *Abstract.*

2.1.2. *Structure determination and refinement.* For the intensity-data collection, an elongated hexagonal platelet measuring $0{\cdot}17 \times 0{\cdot}11 \times 0{\cdot}04$ mm was aligned about $\mathbf{c}^*$ on a Siemens AED single-crystal diffractometer. Operating conditions were θ–2θ scan; 2θ range 5–60°; scan speed $0{\cdot}03°(2\theta)\ s^{-1}$. A total of 4038 reflections were measured for $h = -11$ to 11, $k = -11$ to 11, $l = 0$ to 15. Of these, 1298 reflections in the 2θ range 5–40° were re-collected to check reproducibility, $R_{int} = 0{\cdot}014$. A standard reflection measured every 3 h showed less than 2% intensity variation. The data were corrected for absorption, maximum and minimum transmission coefficients 0.60 and 0·37, and reduced to 3449 unique structure amplitudes, of which 2319 with $I > 3\sigma(I)$ were used in the structure refinement.

A set of coordinates for the Zn atoms in the $Zn(OH)_2$ layer, consistent with the three-dimensional Patterson map, was used to phase a Fourier map in which the S and a number of O atoms were located. Subsequent refinement and difference Fourier syntheses in $P\bar{1}$ revealed all nonhydrogen atoms. The O atoms of two water molecules, $O_w(14)$ and $O_w(15)$ in Table 1, were observed to be disordered between pairs of sites, separated by 1·5 and 0·9 Å respectively. The occupancies of these sites were refined, subject

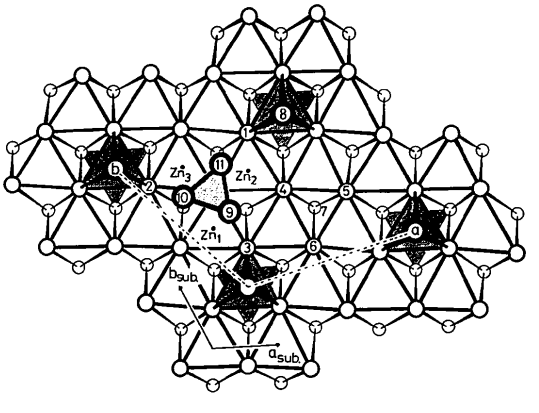

Fig. 1. Polyhedral representation of the modified $Zn(OH)_2$ layers viewed along c. Sulfate tetrahedra have light shading and Zn-centred tetrahedra have dark shading. The anions are labelled according to Tables 1 and 3.

Table 1. $3Zn(OH)_2.ZnSO_4.5H_2O$: *final atomic parameters with e.s.d.'s in parentheses*

$$U_{eq}=\tfrac{1}{3}\sum_i\sum_j U_{ij}a_i^*a_j^*\mathbf{a}_i.\mathbf{a}_j.$$

	Population parameter	x	y	z	U_{eq} (Å^2)
Zn(1)		0·1307 (1)	0·4173 (1)	0·9994 (1)	0·0139 (5)
Zn(2)		0·4146 (1)	0·2858 (1)	0·0077 (1)	0·0146 (5)
Zn(3)		0·7137 (1)	0·1309 (1)	0·0084 (1)	0·0140 (5)
Zn(4)		0·9778 (1)	0·0021 (1)	0·1610 (1)	0·0137 (5)
S		0·3000 (3)	0·6774 (3)	0·2603 (2)	0·016 (1)
$O_H(1)$		0·7390 (7)	0·9446 (7)	0·1091 (5)	0·016 (3)
$O_H(2)$		0·0409 (7)	0·8122 (7)	0·1078 (5)	0·016 (3)
$O_H(3)$		0·1723 (7)	0·2503 (7)	0·1151 (5)	0·013 (3)
$O_H(4)$		0·6153 (7)	0·5280 (7)	0·0843 (5)	0·014 (3)
$O_H(5)$		0·8821 (7)	0·3775 (7)	0·0870 (5)	0·014 (3)
$O_H(6)$		0·4634 (7)	0·1049 (7)	0·0856 (5)	0·014 (3)
O(7)		0·3176 (7)	0·6672 (7)	0·1229 (5)	0·014 (3)
$O_w(8)$		0·9362 (8)	0·9810 (8)	0·3419 (5)	0·036 (4)
O(9)		0·2858 (7)	0·5103 (7)	0·3075 (5)	0·030 (3)
O(10)		0·1297 (8)	0·6901 (8)	0·3017 (5)	0·030 (3)
O(11)		0·4663 (7)	0·8423 (7)	0·3016 (5)	0·022 (3)
$O_w(12)$		0·9720 (9)	0·2859 (9)	0·4577 (6)	0·041 (4)
$O_w(13)$		0·7220 (10)	0·3381 (12)	0·3445 (7)	0·070 (6)
$O_w(14A)$	0·72 (1)	0·3461 (13)	0·1170 (14)	0·3531 (10)	0·059 (7)
$O_w(14B)$	0·28	0·4276 (46)	0·1085 (42)	0·4757 (25)	0·10 (2)
$O_w(15A)$	0·55 (4)	0·6700 (16)	0·6209 (18)	0·3481 (13)	0·045 (8)
$O_w(15B)$	0·45	0·3455 (25)	0·3326 (25)	0·5741 (14)	0·051 (11)

to the constraint that the sum of the partial occupancies of the pairs of sites was 1·0. After refinement of coordinates and anisotropic temperature factors, the H atoms were located in a difference Fourier map. With H atoms included but not refined, the final wR and R factors for the 2319 reflections with $I>3\sigma(I)$ were 0·031 and 0·042. 201 parameters were refined (on F), using $1/\sigma(F)^2$ weights where $\sigma(F)=\sigma(I)/2F\text{Lp}$. The maximum Δ/σ was 0·18. $(\Delta\rho)_{max}=|1\cdot0|$e Å^{-3}, wR and R for all reflections were 0·078 and 0·041. No correction for secondary extinction. Scattering factors for neutral atoms were taken from *International Tables for X-ray Crystallography* (1974) and computing programs used were *SHELX*76 (Sheldrick, 1976) and *ORTEP*II (Johnson, 1976). Final coordinates and equivalent isotropic thermal parameters are given in Table 1 and important bond lengths and angles are listed in Table 2.*

2.2. *Dehydration of* $3Zn(OH)_2.ZnSO_4.5H_2O$

Powder XRD, DTA/TG, infrared-spectroscopy studies and chemical analyses of products obtained by controlled dehydration of the pentahydrate over various desiccants at room temperature have revealed the existence of discrete lower hydrates $3Zn(OH)_2.ZnSO_4.mH_2O$, with $m=4$, 3 and 1 (Bear and co-workers, to be published). (Hydrates with $m=2$ and 0·5 were not observed using desiccants to control the water-vapour pressure, but the latter formed when dehydration was carried out by controlled heating.) The tetrahydrate occupies a very narrow stability region and is extremely difficult to prepare in a pure form whereas the trihydrate is stable over a relatively wide water-vapour-pressure range of ~1–5 mm (~10–50 Pa).

We studied the dehydration of pentahydrate single crystals to the trihydrate using the precession method. Nitrogen gas, which was first bubbled through 54% H_2SO_4, was blown onto the mounted crystal to maintain the required vapour pressure. It was found that coating the crystal with Apiezon vacuum grease slowed down the dehydration reaction and this allowed the formation of the tetrahydrate as an intermediate phase to be recorded in a series of precession photographs. These could be indexed using an I-centred triclinic cell with pseudohexagonal geometry, $a\simeq b\simeq 8\cdot35$, $c\simeq 20\cdot70$ Å (*i.e.* $2\times10\cdot35$ Å), $\alpha\simeq\beta\simeq 90$, $\gamma\simeq 120°$. On further dehydration to the trihydrate, the pseudohexagonal I-centred cell was maintained, with similar a and b parameters but with a reduction in c to $2\times9\cdot28=18\cdot56$ Å.

The precession study showed that the dehydration reactions were accompanied by three types of modifications to the layer structures that were all deleterious to the quality of the intensity data for a structure refinement. Firstly, the dehydrated crystals were twinned, with the pseudohexagonal subcell symmetry elements as twin laws. Secondly, tilting and misorientation of layers occurred, as shown by arcing of reflections. This was most severe in the $[1\bar{1}0]$-zone diffraction pattern where the arcing occurred over ~3–5°. Thirdly, a gradual breakdown in the long-range ordering between layers along **c** with increasing dehydration was evidenced by a progressive and marked decrease in the average intensities of the $00l$ reflections relative to the subcell $hk0$ reflections.

2.3. *Structure of* $3Zn(OH)_2.ZnSO_4.3H_2O$

For the intensity-data collection, a crystal was chosen that appeared to be free of twinning. It was in the form of a hexagonal platelet, 0·10 mm on edge and 0·04 mm thick. The crystal was mounted along **c*** on the Siemens AED diffractometer, and an intensity-data set collected in the 2θ range 5–50° using the same conditions as described above for the pentahydrate.

Unit-cell parameters, refined using the 2θ values of 62 powder-pattern reflections in the range 9–65° (Cu $K\alpha$ radiation), are given in the *Abstract*. A total of 1999 reflections were measured for h and $k=-9$ to 9 and $l=0$ to 20. The data were corrected for absorption, maximum and minimum transmission factors 0·54 and 0·29, and reduced to 1725 unique structure amplitudes, $R_{int}=0\cdot029$, of which 1120 had $I>3\sigma(I)$ and were used in the refinement.

* Lists of anisotropic thermal parameters, H-atom coordinates and structure factors have been deposited with the British Library Lending Division as Supplementary Publication No. SUP42438 (29 pp.). Copies may be obtained through The Executive Secretary, International Union of Crystallography, 5 Abbey Square, Chester CH1 2HU, England.

The Zn coordinates from the refinement of the pentahydrate phase were used as starting coordinates in $I\bar{1}$ and the S and O atoms were located by Fourier methods. Refinement of all coordinates and anisotropic temperature factors led to convergence at $wR = 0{\cdot}13$ for the 1120 observed reflections with $I > 3\sigma(I)$. A comparison of observed and calculated structure amplitudes showed that the F_{obs} were systematically greater than F_{calc} for the $hk0$ reflections. The difference decreased with increasing l component and for the $00l$ reflections the F_{obs} were systematically weaker than the F_{calc}. The difference Fourier map showed a set of peaks corresponding to a weak image of the structure, displaced along **c** by $\Delta z = \pm 0{\cdot}06$ (1.1 Å). These observations are consistent with partial disorder of the layer structure, *e.g.* due to small randomly intergrown regions of higher and/or lower hydrates, giving uncorrelated layer spacings of different periodicities. It is worth noting that the displacement of the ghost images of the structure along **c**, 1·1 Å, corresponds to the change in layer spacing from the tetrahydrate (10·35 Å) to the trihydrate (9·28 Å). In spite of the high R factors due to the disorder, the structure of the trihydrate was considered to be well determined as evidenced by the lack of features other than the ghost image in the final Fourier map, and by the reasonable bond lengths obtained from the refined coordinates.

Final coordinates and isotropic thermal parameters are given in Table 3. Bond lengths and angles are listed in Table 2.*

Table 2. *Bond lengths* (Å) *and angles* (°) *in* $3Zn(OH)_2.ZnSO_4.5H_2O$ (I) *and* $3Zn(OH)_2.ZnSO_4.3H_2O$ (II)

Zn(1) octahedron

	(I)	(II)		(I)	(II)
Zn(1)–O(4)	2·044 (5)	2·02 (3)	Zn(1)–O(2)	2·108 (6)	2·13 (3)
–O(5)	2·055 (5)	2·09 (3)	–O(3)	2·133 (5)	2·15 (4)
–O(5')	2·076 (6)	2·12 (3)	–O(7)	2·340 (6)	2·27 (3)

	(I)	(II)	(I)	(II)
O(4)–O(5)	3·060 (8)	3·07 (4)	95·9 (2)	95·4 (1·3)
–O(2)	3·171 (8)	3·16 (5)	99·5 (2)	99·3 (1·3)
–O(3)	2·789 (7)	2·79 (4)	83·8 (2)	83·7 (1·2)
–O(7)	2·862 (8)	2·88 (6)	81·2 (2)	84·0 (1·3)
O(5)–O(5')	2·718 (10	2·80 (7)	83·2 (2)	83·3 (1·3)
–O(2)	2·770 (7)	2·81 (5)	83·4 (2)	83·6 (1·3)
–O(3)	3·147 (8)	3·18 (5)	97·4 (2)	97·1 (1·3)
–O(7)	3·267 (8)	3·17 (4)	95·8 (2)	93·2 (1·2)
–O(2)	3·183 (8)	3·17 (4)	99·0 (2)	96·6 (1·3)
–O(7)	2·906 (7)	2·94 (5)	82·1 (2)	83·8 (1.3)
O(2)–O(3)	3·067 (8)	3·08 (5)	92.6 (2)	91.9 (1·3)
O(3)–O(7)	3·060 (8)	3·06 (4)	86·2 (2)	87·6 (1·3)

Zn(2) octahedron

	(I)	(II)		(I)	(II)
Zn(2)–O(6)	2.020 (6)	2.05 (3)	Zn(2)–O(3)	2.109 (5)	2.09 (4)
–O(4)	2·049 (6)	2·07 (4)	–O(1)	2·135 (5)	2·16 (4)
–O(4')	2·077 (5)	2·09 (3)	–O(7)	2·376 (5)	2·40 (3)

	(I)	(II)	(I)	(II)
O(6)–O(4)	3·102 (8)	3·10 (4)	98·4 (2)	96·9 (1·2)
–O(3)	3·191 (8)	3·18 (5)	101·2 (2)	100·5 (1.4)
–O(1)	2·770 (7)	2·83 (4)	83·6 (2)	84·4 (1·3)
–O(7)	2·898 (8)	2·93 (4)	82·0 (2)	82·1 (1·3)
O(4)–O(4')	2·686 (11)	2·75 (7)	81·2 (2)	82·8 (1.5)
–O(3)	2·789 (7)	2·79 (4)	84·3 (2)	84·3 (1·2)
–O(1)	3·095 (8)	3·11 (4)	95·4 (2)	94·6 (1·4)
–O(7)	3·204 (8)	3·25 (4)	92·5 (2)	93·0 (1·4)
–O(3)	3·231 (7)	3·23 (5)	101·0 (2)	101·2 (1·5)
–O(7)	2·862 (8)	2·88 (5)	79·7 (2)	79·4 (1.3)
O(3)–O(1)	3·069 (8)	3·09 (5)	92·6 (2)	93·4 (1·4)
O(1)–O(7)	3·093 (8)	3·11 (4)	86·4 (2)	85·8 (1·4)

Zn(3) octahedron

	(I)	(II)		(I)	(II)
Zn(3)–O(5)	2·025 (5)	2·04 (3)	Zn(3)–O(1)	2·084 (6)	2·05 (3)
–O(6)	2·069 (5)	2·04 (3)	–O(2)	2·131 (5)	2·13 (3)
–O(6')	2·071 (5)	2·13 (4)	–O(7)	2·430 (5)	2·50 (3)

	(I)	(II)	(I)	(II)
O(5)–O(6)	3·079 (7)	3·04 (4)	97·5 (2)	96·6 (1·3)
–O(1)	3·211 (8)	3·21 (4)	102·7 (2)	103·5 (1·4)
–O(2)	2·770 (7)	2·81 (4)	83·5 (2)	84·7 (1·4)
–O(7)	2·906 (8)	2·94 (4)	80·9 (2)	79·8 (1·3)
O(6)–O(6')	2·696 (11)	2·76 (7)	81·3 (2)	82·7 (1·2)
–O(1)	3·230 (7)	3·21 (4)	102·1 (2)	103·3 (1·3)
–O(7)	2·898 (7)	2·93 (4)	79·7 (2)	79·7 (1·3)
–O(1)	2·770 (7)	2·83 (4)	83·6 (2)	85·1 (1·3)
–O(2)	3·125 (8)	3·10 (4)	96·0 (2)	93·3 (1·4)
–O(7)	3·268 (7)	3·32 (4)	92·7 (2)	91·4 (1·4)
O(1)–O(2)	3·024 (7)	3·05 (4)	91·7 (2)	93·7 (1·3)
O(2)–O(7)	3·123 (8)	3·08 (4)	86·1 (2)	82·9 (1·3)

Zn(4) tetrahedron

	(I)	(II)		(I)	(II)
Zn(4)–O(2)	1·937 (5)	1·96 (3)	Zn(4)–O(1)	1·954 (5)	1·96 (3)
–O(3)	1·947 (5)	1·96 (3)	–O(8)	1·983 (5)	1·83 (6)

	(I)	(II)	(I)	(II)
O(2)–O(3)	3·250 (7)	3·23 (4)	113·6 (2)	111·2 (1·4)
–O(1)	3·218 (8)	3·31 (4)	111·6 (2)	115·5 (1·4)
–O(8)	3·082 (7)	3·03 (6)	103·7 (2)	106·3 (1·6)
O(3)–O(1)	3·231 (7)	3·23 (5)	111·8 (2)	111·4 (1·4)
–O(8)	3·224 (7)	3·05 (6)	110·3 (2)	107·4 (1·6)
O(1)–O(8)	3·127 (8)	2·99 (6)	105·2 (2)	104·2 (1·6)

Table 2 (*cont.*)

S tetrahedron

	(I)	(II)		(I)	(II)
S–O(11)	1·478 (5)	1·49 (3)	S–O(10)	1·491 (6)	1·44 (3)
–O(9)	1·471 (6)	1·47 (3)	–O(7)	1·501 (6)	1·48 (4)

	(I)	(II)	(I)	(II)
O(11)–O(9)	2·407 (7)	2·41 (4)	109·5 (4)	108·8 (2·2)
–O(10)	2·441 (7)	2·42 (5)	110·6 (4)	111·1 (2·1)
–O(7)	2·426 (7)	2·41 (5)	109·2 (3)	108·6 (2·0)
O(9)–O(10)	2·439 (8)	2·40 (4)	110·8 (3)	111·1 (2·4)
–O(7)	2·416 (7)	2·40 (6)	108·8 (4)	109·0 (2·2)
O(10)–O(7)	2·419 (7)	2·37 (6)	107·9 (3)	108·2 (2·3)

Table 3. $3Zn(OH)_2.ZnSO_4.3H_2O$: *final atomic parameters with e.s.d.'s in parentheses*

$$U_{eq} = \tfrac{1}{3}\sum_i\sum_j U_{ij}a_i^* a_j^* \mathbf{a}_i.\mathbf{a}_j.$$

	x	y	z	U_{eq}
Zn(1)*	0·1330 (8)	0·4184 (7)	0·0000 (4)	0·029 (3)
Zn(2)	0·4167 (8)	0·2866 (7)	0·0041 (4)	0·027 (3)
Zn(3)	0·7146 (8)	0·1285 (7)	0·0088 (4)	0·028 (3)
Zn(4)	0·9977 (7)	0·9936 (7)	0·0944 (4)	0·024 (3)
S	0·3189 (16)	0·6639 (15)	0·1516 (7)	0·023 (6)
$O_H(1)$	0·750 (4)	0·942 (4)	0·067 (2)	0·03 (2)
$O_H(2)$	0·062 (4)	0·810 (4)	0·063 (2)	0·03 (3)
$O_H(3)$	0·189 (4)	0·243 (4)	0·066 (2)	0·04 (3)
$O_H(4)$	0·630 (4)	0·528 (4)	0·051 (2)	0·04 (2)
$O_H(5)$	0·896 (4)	0·376 (4)	0·055 (2)	0·02 (2)
$O_H(6)$	0·479 (4)	0·106 (4)	0·052 (2)	0·03 (2)
O(7)	0·327 (4)	0·658 (4)	0·072 (2)	0·02 (2)
$O_w(8)$	0·991 (4)	0·986 (4)	0·192 (3)	0·08 (3)
O(9)	0·289 (5)	0·488 (4)	0·181 (2)	0·05 (3)
O(10)	0·169 (5)	0·693 (5)	0·171 (2)	0·05 (2)
O(11)	0·500 (4)	0·818 (5)	0·178 (2)	0·03 (2)
$O_w(14)$	0·502 (6)	0·138 (5)	0·209 (3)	0·08 (3)
$O_w(15)$	0·747 (6)	0·515 (5)	0·199 (2)	0·05 (2)

* Atom labels correspond to equivalent labels in Table 1.

* See deposition footnote.

3. Description of the structures

3.1. *Octahedral layer structure*

The structures of $3Zn(OH)_2.ZnSO_4.3H_2O$ and $3Zn(OH)_2.ZnSO_4.5H_2O$ are closely related, being both based on an alternation along **c** of modified octahedral layers and layers containing water molecules and sulfate-group O atoms.

The modified $Zn(OH)_2$ layer common to both structures is illustrated in Fig. 1. One-seventh of the octahedral sites are vacant, forming a $\sqrt{7}a_{subcell}$ superstructure of the 3·15 Å α-$Zn(OH)_2$ structure. Tetrahedrally coordinated Zn atoms are located above and below the empty octahedra and corner-share their basal anions (hydroxides) with six octahedra. The apices of the tetrahedra are water molecules. Sulfate tetrahedra are also linked to either side of the octahedral layers by corner-sharing *via* their apical O atoms. The composition of the octahedral layer is $[Zn_6\square(OH)_{12}O_2]^{4-}$ and the composition of the complete layer, which is neutral, is $[Zn_6^{VI}\square(OH)_6.Zn_2^{IV}(OH)_6(H_2O)_2.(SO_4)_2]$. The alternation of these layers with layers of water molecules along **c** is illustrated in Figs. 2 and 3 for the pentahydrate and the trihydrate respectively.

In the pentahydrate, successive octahedral layers are aligned almost vertically, *i.e.* the Zn tetrahedra are almost directly above and below one another in adjacent layers, whereas in the trihydrate successive layers are displaced by $\frac{1}{2}[\mathbf{a}+\mathbf{b}]$. The sulfate tetrahedra have the same orientation in the two structures, which is maintained by hydrogen bonding to the hydroxyls of the octahedral layers.

Polyhedral bond lengths and angles for the two hydrates are compared in Table 2. The geometry of the modified $Zn(OH)_2$ layer is virtually identical for the two structures. The bonding of the sulfate group to the octahedral framework results in oversaturation of the shared O atom, O(7), and the bonds of O(7) to the octahedrally coordinated Zn atoms, Zn(1) to Zn(3), in the range 2·27–2·50 Å for the trihydrate and 2·34–2·43 Å for the pentahydrate, are much longer than the other bonds. The mean octahedral Zn–O bond lengths of 2·14(3) Å for the trihydrate and 2·130(5) Å for the pentahydrate are comparable with values for other basic Zn salts, *e.g.* 2·13 Å in $4Zn(OH)_2.Zn(NO_3)_2.2H_2O$ (Stählin & Oswald, 1970), 2·16 Å in $4Zn(OH)_2.ZnCl_2.H_2O$ (Allmann, 1968) and 2·10 Å in $3Zn(OH)_2.2ZnCO_3$ (Ghose, 1964). The mean Zn(4)–O tetrahedral distance, 1·93(4) Å for the trihydrate and 1·955(6) Å for the pentahydrate, compares with corresponding values of 1·95, 1·94 and 1·95 Å for the above three compounds. The shorter mean Zn(4)–O distance for the trihydrate is due to an unusually short bond to the apical water O atom, Zn(4)–O_w(8) 1·83(6) Å. This O has a very large anisotropic thermal component [$U_{33}=0{\cdot}22(6)$] along **c**, the direction of the Zn(4)–O_w(8) bond, and is considered to result from the refinement attempting to compensate for the disorder.

3.2. *The interlayer region*

The interlayer region consists of the basal O atoms, O(9)–O(11), of the sulfate tetrahedra, the coordinated water molecule O_w(8) that forms the apex of the Zn tetrahedra, and free water molecules. The packing of these components is illustrated in Figs. 4 and 5 for the pentahydrate and trihydrate respectively.

In the pentahydrate, the water molecules and O atoms form approximately close-packed layers. For comparison an ideal close-packed network is shown by the dashed lines in Fig. 4. Pairs of such layers, related by the inversion centre, are separated by about 3·6 Å. This large spacing is maintained by an interlayer water molecule, O_w(12), that occupies a tetrahedral site formed by a sulfate O atom, O(9), and two water molecules, O_w(8) and O_w(13), from one layer and a sulfate O atom, O(10), from the second layer. The tetrahedral O–O bonds are all short, 2·65–2·78 Å,

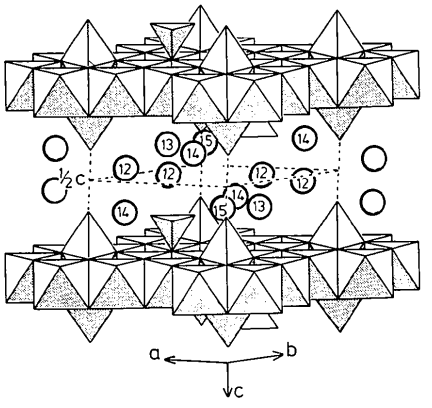

Fig. 2. The structure of $3Zn(OH)_2.ZnSO_4.5H_2O$, viewed approximately along [110]. Circles represent water molecules, labelled according to Table 1. Only sites *A* of the disordered molecules O_w(14) and O_w(15) are shown for clarity.

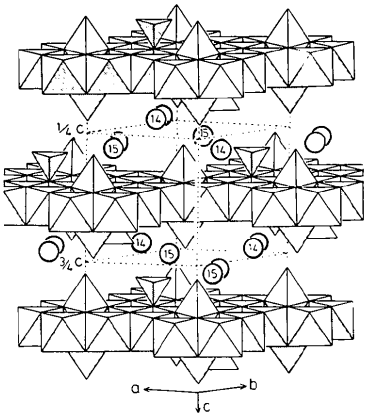

Fig. 3. The structure of $3Zn(OH)_2.ZnSO_4.3H_2O$, viewed approximately along [110].

indicative of strong hydrogen bonding, which is the main force holding the layers together. The disordered water molecules, $O_w(14)$ and $O_w(15)$, also partially occupy the region between the pairs of close-packed layers when in sites 14*B* and 15*B*, as shown in Fig. 4.

In the trihydrate, the sulfate O atoms and water molecules also form pairs of approximately close-packed layers, but with a vacant site per unit-cell layer, as shown in Fig. 5. The interlayer-type water molecule $O_w(12)$, found in the pentahydrate, is absent in the trihydrate, allowing the layer separation to contract from 3·6 to about 2·3 Å, becoming comparable to the anion-layer separation of 2·2 Å in the octahedral layer.

In both the penta- and the trihydrates, the close-packed layers of water molecules and sulfate O atoms are rotated by ~22° relative to the adjacent array of the octahedral layer (compare Figs. 4 and 5 with Fig. 1). The orientation of the two types of layers can be brought into coincidence by a 180° rotation about an axis parallel to $[1\bar{1}0]$. The orientation adopted by the close-packed layers of waters and O atoms is controlled by the orientation of the triangle of sulfate basal O atoms, which in turn is maintained by strong hydrogen bonding with the three basal hydroxyls of the Zn tetrahedra, $O_H(1)$-$O_H(3)$ in Table 2.

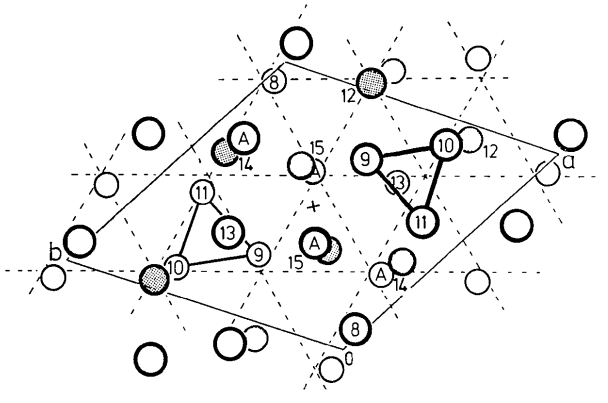

Fig. 4. Section through the interlayer region in $3Zn(OH)_2.ZnSO_4.5H_2O$. Connected triangular groupings are sulfate O atoms. Layers at $z \approx 0{\cdot}33$ and 0·67 shown by small and large circles respectively. Interlayer water molecules $O_w(12)$, $O_w(14B)$ and $O_w(15B)$ are shaded. An ideal hexagonal network at $z = 0{\cdot}33$ is shown by dashed lines. The unit-cell outline at $z = 0{\cdot}5$ is given.

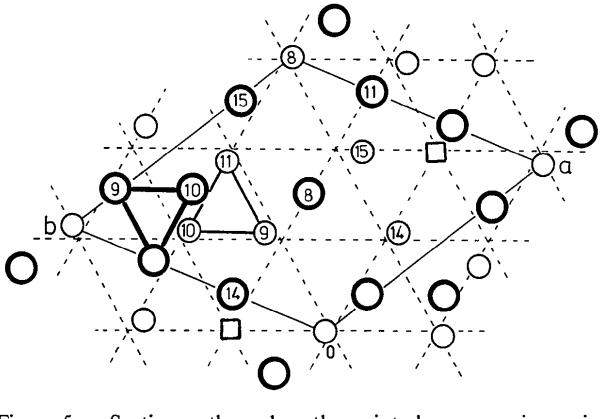

Fig. 5. Section through the interlayer region in $3Zn(OH)_2.ZnSO_4.3H_2O$. Layers at $z \approx 0{\cdot}19$ and 0·31 shown by small and large circles respectively, □ = vacant anion site.

Table 4. *Hydrogen-bonded* O–O *distances* (Å) *in* $3Zn(OH)_2.ZnSO_4.5H_2O$ *and* $3Zn(OH)_2.ZnSO_4.3H_2O$

Bonds involving hydroxyls

$3Zn(OH)_2.ZnSO_4.5H_2O$		$3Zn(OH)_2.ZnSO_4.3H_2O$	
$O_H(1)$–O(11)	2·749 (7)	$O_H(1)$–O(11)	2·74 (5)
$O_H(2)$–O(10)	2·760 (8)	$O_H(2)$–O(10)	2·60 (6)
$O_H(3)$–O(9)	2·797 (7)	$O_H(3)$–O(9)	2·77 (6)
$O_H(4)$–$O_w(15A)$	2·976 (8)	$O_H(4)$–$O_w(15)$	2·94 (6)
$O_H(5)$–$O_w(13)$	2·949 (7)	$O_H(6)$–$O_w(14)$	2·92 (7)
$O_H(6)$–$O_w(14A)$	2·996 (7)		

Bonds involving water molecules

	Intralayer		Interlayer
$3Zn(OH)_2.ZnSO_4.5H_2O$			
$O_w(8)$–$O_w(15A)$	2·70 (2)	$O_w(8)$–$O_w(15B)$	2·63 (2)
–$O_w(14A)$	3·04 (2)	–$O_w(12)$	2·65 (2)
$O_w(13)$–$O_w(15A)$	2·60 (2)	$O_w(12)$–O(10)	2·70 (1)
–$O_w(14A)$	2·73 (1)	–O(9)	2·76 (1)
$O_w(14A)$–O(11)	2·92 (2)	–$O_w(13)$	2·78 (1)
$O_w(15A)$–O(9)	2·95 (2)	$O_w(13)$–$O_w(14B)$	2·58 (3)
		–$O_w(15B)$	3·12 (3)
		$O_w(14A)$–$O_w(15B)$	2·93 (3)
		$O_w(14B)$–$O_w(15B)$	2·43 (3)
		–O(11)	2·64 (3)
		$O_w(15B)$–O(9)	3·10 (2)
		–O(11)	3·10(2)
$3Zn(OH)_2.ZnSO_4.3H_2O$			
$O_w(14)$–O(11)	2·74 (5)	$O_w(8)$–$O_w(15)$	2·82 (5)
–$O_w(15)$	2·77 (5)	–O(9)	2·93 (5)
$O_w(15)$–O(10)	3·09 (5)	$O_w(14)$–O(9)	2·93 (5)
		$O_w(15)$–O(11)	2·94 (5)

3.3. *Hydrogen-bond system*

All H atoms except those associated with the disordered atom component $O_w(14B)$ were located in the refinement of the pentahydrate. The poor quality of the intensity data for the trihydrate prevented their location in the refinement, but the similarity of the two structures suggests that the hydrogen-bond systems will be closely related. A list of O–O bonds corresponding to hydrogen bonding for both hydrates is given in Table 4. The following discussion refers to the results obtained for the pentahydrate.

The three hydroxyls forming the base of the Zn(4)-$(OH)_3H_2O$ tetrahedron, $O_H(1)$-(3), are each involved in hydrogen bonding to the basal O atoms of the sulfate molecules, O(9)-(11), with corresponding O–O distances in the range 2·75–2·80 Å. The remaining hydroxyls, $O_H(4)$-(6), form weak hydrogen bonds to the interlayer water molecules, $O_w(13)$-(15), with O–O distances in the range 2·95–3·00 Å. The H atoms associated with the interlayer water molecules $O_w(8)$, $O_w(13)$ and $O_w(14)$ were found to be disordered over a number of positions, as illustrated in Fig. 6(*a*). The

disorder in the position of the water molecule $O_w(15)$ over the two sites 15*A* and 15*B* is related to the statistically distributed H atoms on $O_w(8)$ in a similar way to the case described in detail for the disordered water molecules in $Na_3[Ce(C_4H_4O_5)_3].9H_2O$ (Albertsson & Elding, 1976). That is, when $O_w(15)$ is in position *A*, it acts as an acceptor of a hydrogen bond from $O_w(8)$, and as a donor to the sulfate O atom O(9) and water molecule $O_w(13)$. When it is in position *B*, it reverses roles with $O_w(8)$ and donates a hydrogen bond to the latter. The disorder of $O_w(14)$ is also presumably related to the change of hydrogen-bonding patterns, but not all details have been determined because the H atoms associated with the minor component, $O_w(14B)$, were not located. An example of one of the possible ordering schemes contributing to the observed statistical distribution is shown in Fig. 6(*b*).

4. Discussion

The structures of the 3:1 basic zinc sulfates appear to be the first reported examples of basic salts comprising $M(OH)_2$ octahedral layers with ordered octahedral vacancies in the ratio 1:6. The hydrated oxide mineral chalcophanite, $ZnMn_3O_7.3H_2O$, contains $[Mn_6\square O_{14}]^{4-}$ octahedral layers with the same vacancy:occupied-site ratio of 1:6 (Wadsley, 1955). In this case $[ZnO_3(H_2O)_3]^{4-}$ octahedra are located above and below the vacant sites. There have been reported a number of basic Zn salts of general formula $4Zn(OH)_2.ZnX_2.nH_2O$, $X=NO_3$ (Stählin & Oswald, 1970) and Cl (Allmann, 1968) and $3Zn(OH)_2.2ZnX$, $X=CO_3$ (Ghose, 1964), that have a vacancy:occupied-site ratio of 1:3 in the octahedral layers and with tetrahedrally coordinated Zn above and below the vacancies. The only other reported basic zinc sulfate structure, $Zn(OH)_2.ZnSO_4$ (Iitaka, Oswald & Locchi, 1962), does not contain analogous $Zn(OH)_2$ octahedral layers. Instead, the Zn-centred octahedra form edge-shared chains which are linked *via* corner-sharing with zigzag chains of corner-shared tetrahedra. However, the mixed Zn/Mg/Mn basic sulfates mooreite (Hill, 1980) and lawsonbauerite (Treiman & Peacor, 1982) have structural features in common with the basic sulfates described here. Hill (1981) has recently discussed the crystal chemistry of a range of related basic salts consisting of sheets of edge-shared octahedra containing a variable number of vacant metal-atom sites. A recently reported addition to this list is the mineral langite, $3Cu(OH)_2.CuSO_4.2H_2O$, which has the same ratio of hydroxide to sulfate as the Zn compounds reported here. However, a structure refinement (Gentsch & Weber, 1984) shows that the octahedral layers are fully occupied in this compound, giving a layer composition $[Cu_4(OH)_6(H_2O)O]$ where the O is corner-shared with sulfate groups as in $3Zn(OH)_2.ZnSO_4.mH_2O$.

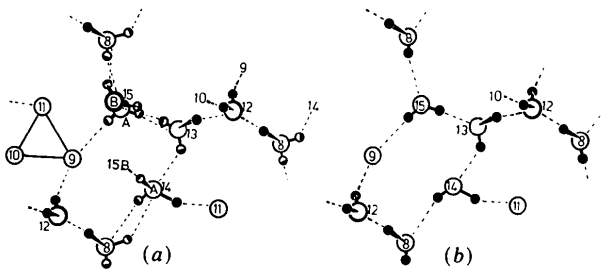

Fig. 6. Hydrogen bonding in the interlayer region for $3Zn(OH)_2.ZnSO_4.5H_2O$, showing atoms close to $z=0.33$. (*a*) Statistical distribution of H atoms determined from the refinement. $O_w(14B)$ not shown as H atoms were not located. (*b*) One of the ordered arrangements consistent with (*a*).

4.1. *Dehydration mechanism*

The major changes accompanying the removal of water on dehydration of $3Zn(OH)_2.ZnSO_4.5H_2O$ are a reduction of the interlayer spacing (by ~0·65 Å on forming the tetrahydrate and a further 1·1 Å on dehydration to the trihydrate), and a sliding of the layers relative to one another by $\frac{1}{2}(\mathbf{a}+\mathbf{b})\simeq 4{\cdot}2$ Å. Such large atomic movements are not fully cooperative at room temperature as indicated by the considerable disorder in the structure of the trihydrate. The observation of twinning in the dehydration product, controlled by the underlying pseudohexagonal substructure, indicates that rotation of adjacent layers by ±60° can also occur during the dehydration. The precession studies showed that the intermediate tetrahydrate phase had the same *I*-centred pseudohexagonal cell as that of the trihydrate, implying that the major parallel movement of the layers relative to one another occurs during the removal of the first water molecule. Subsequent elimination of a second water molecule results mainly in a further collapse of the structure perpendicular to the layers.

The atomic movements that accompany the dehydration can be elucidated from a comparison of Figs. 4 and 5. If attention is focused on equivalent layers, *i.e.* at $z\simeq 0{\cdot}33$ and $z\simeq 0{\cdot}19$ for the pentahydrate and trihydrate respectively, it is seen that the orientation of the sulfate tetrahedra and the positions of the water molecules $O_w(8)$, $O_w(14)$ and $O_w(15)$ are only changed slightly. The dehydration has involved the loss of the water molecule $O_w(13)$ from the close-packed layer, and the water molecule $O_w(12)$ from between the layers. From the observation that the **c** axis decreases by only 0·65 Å due to the loss of the first water molecule and then by 1·07 Å on the loss of the second, we conclude that $O_w(13)$ is lost in the formation of the tetrahydrate, leaving $O_w(12)$ in an interlayer site. Consistent with this, $O_w(13)$ is found to have the largest anisotropic thermal parameter of all atoms, $U(22)=0{\cdot}111(7)$.

References

ALBERTSSON, J. & ELDING, J. (1976). *Acta Cryst.* B32, 3066-3077.
ALLMANN, R. (1968). *Z. Kristallogr.* **126**, 417-426.
FEITKNECHT, W. (1933*a*). *Z. Kristallogr.* **84**, 173-176.
FEITKNECHT, W. (1933*b*) *Helv. Chim. Acta*, **16**, 427-454.
FRIDMAN, G. B. (1935). *Zh. Prikl. Khim. (Leningrad)*, **8**, 227-239.
GENTSCH, M. & WEBER, K. (1984). *Acta Cryst.* C40, 1309-1311.
GHOSE, S. (1964). *Acta Cryst.* **17**, 1051.
HILL, R. J. (1980). *Acta Cryst.* B36, 1304-1311.
HILL, R. J. (1981). *Acta Cryst.* B37, 1323-1328.
IITAKA, V., OSWALD, H. R. & LOCCHI, S. (1962). *Acta Cryst.* **15**, 559-563.
International Tables for X-ray Crystallography (1974). Vol. IV. Birmingham: Kynoch Press. (Present distributor D. Reidel, Dordrecht.)
JACOB, M. & RIQUIER, J. (1969). *J. Metall.* **9**, 127.
JOHNSON, C. K. (1976). *ORTEP*II. Report ORNL-5138. Oak Ridge National Laboratory, Tennessee.
KUHN, O. B. (1830). *J. Schweigger's*, **60**, 337.
PASCAL, P. (1962). *Nouveau Traité de Chimie Minérale.* Vol. V. Paris: Masson.
REINDEL, F. (1869). *J. Prakt. Chem.* **106**, 371.
SHELDRICK, G. M. (1976). *SHELX*76. A program for crystal structure determination. Univ. of Cambrige, England.
STÄHLIN, W. & OSWALD, H. R. (1970). *Acta Cryst.* B26, 860-863.
TREIMAN, A. H. & PEACOR, D. R. (1982). *Am. Mineral.* **67**, 1029-1034.
WADSLEY, A. D. (1955). *Acta Cryst.* **8**, 165-172.

Acta Cryst. (1986). B42, 39-43

The Imaging of Individual Cation Columns in f.c.c. Mixed Alloy Systems

By O. TERASAKI*

Department of Physical Chemistry, University of Cambridge, Lensfield Road, Cambridge, England

DAVID J. SMITH† AND G. J. WOOD†

High Resolution Electron Microscope, University of Cambridge, Free School Lane, Cambridge, England

(*Received* 4 *September* 1984; *accepted* 22 *August* 1985)

Abstract

Electron micrographs of an f.c.c. Au-Mn alloy, of nominal composition $Au_{79}Mn_{21}$, recorded at 500 kV and better than 2 Å point resolution, have demonstrated that it is possible to distinguish between *different* atomic columns of this material in thin specimen regions. These results have been confirmed by computer simulations which indicate that the conditions for imaging, namely the specimen thickness and the objective-lens defocus, are not critical. Some experimental images suggest that the occupation probability of separate columns in the beam direction might be determined although the sensitivity of the technique has not been examined. A small region of a novel superstructure, $Au_{14}Mn_4$, has been observed.

1. Introduction

Binary alloys, of the general formula $A_{1-x}B_x(x \leq \frac{1}{2})$, form a complex variety of superlattice structures, many of which have been investigated using the techniques of high-resolution electron microscopy (HREM) (for a recent review, see Watanabe & Terasaki, 1984). The basic structure of these alloys can be found by the usual diffraction methods so that the problem of determining their complete unit-cell structure is reduced to that of establishing the arrangement of *B* atoms. For superlattices based on the f.c.c. lattice, the projected atomic structure along the [001] zone axis can be represented as shown in Fig. 1. Since the basic unit-cell dimensions for most alloys are typically *ca* 4 Å, then microscope resolutions of better than 2 Å are required to separate columns (1) and (2) and better than 2·8 Å to separate columns (1) and (3). It should be noted that, despite a difference in projected separation, the atoms in columns (2) and (3) are equivalent nearest neighbours to those in column (1).

In order to form an ordered alloy structure, the interaction between nearest-neighbour *B* atoms should be repulsive. Thus, when the concentration of *B* atoms is $\frac{1}{4}$ or less, no nearest-neighbour *B*-*B* pairs are likely to exist. In this case, it is not necessary to resolve the fundamental lattice and both bright- and

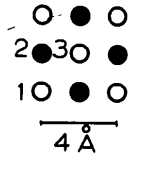

Fig. 1. Schematic showing the basic f.c.c. unit-cell structure of a binary alloy projected along [001]. Filled and empty circles are at different levels within the unit cell.

* Permanent address: Department of Physics, Faculty of Science, Tohoku University, Sendai 980, Japan.

† Present address: Centre for Solid State Science, Arizona State University, Tempe, AZ 85287, USA.

0108-7681/86/010039-05$01.50